Contribution from the Department of Chemistry,
Texas A&M University, College Station, Texas 77843-3255

Crystal and Molecular Structure of the (μ-Hydroxo)dicopper(II) O-BISTREN Complex $Cu_2(OH)(C_{24}O_3N_8H_{54})Br_3 \cdot 6H_2O$

Ramunas J. Motekaitis, Philip R. Rudolf, Arthur E. Martell,* and Abraham Clearfield

Received March 31, 1988

The structure of $Cu_2(\mu\text{-}OH)(O\text{-}BISTREN)Br_3$ has been determined. $Cu_2(OH)(O\text{-}BISTREN)Br_3 \cdot 6H_2O$ crystallizes in space group *C*2/*c* with cell parameters $a = 15.793$ (3) Å, $b = 11.100$ (5) Å, $c = 24.506$ (6) Å, $\beta = 90.92$ (2)°, $V = 4296$ (2) Å^3, $Z = 4$, and $M_r = 994.64$. $R_F = 0.053$ for 2551 observed reflections with $I > 2\sigma(I)$ and 341 variables. The structure comprises the cryptate O-BISTREN ligand encapsulating a Cu–OH–Cu unit. Each copper has distorted-trigonal-prismatic geometry that includes four nitrogens and the hydroxo oxygen. The Cu–O(H)–Cu angle is 155.5 (4)°. The hydroxo hydrogen points at a single O-BISTREN ether oxygen rather than being disordered over the three ether oxygen bridges. The hydroxo oxygen and hydrogen, together with this one O-BISTREN ether oxygen, lie on a 2-fold axis, fixing the geometry of the bridge. The water and bromine atoms are located between O-BISTREN molecular units and are involved in hydrogen bonding between adjacent molecules. The hydrogen bonding of the μ-hydroxo group to an ether oxygen bridge confirms the predictions previously made on the basis of solution thermodynamic data.

Introduction

Potentiometric studies of the dinuclear copper(II)–O-BISTREN cryptate[1-4] (O-BISTREN = 7,19,30-trioxa-1,4,10,13,16,22,27,33-octaazabicyclo[11.11.11]pentatriacontane; it was formerly termed BISTREN) revealed the unusual nature of the μ-hydroxo bridge between the copper(II) ions, to form a monohydroxo dinuclear cryptate species that dominates the solution chemistry of the Cu(II)–O-BISTREN system over a very wide pH range (4–11). The hydroxide binding constant for Cu_2(O-BISTREN) is $10^{10.0}$, compared to the binding constant of the isoelectronic fluoride ion of $10^{4.5}$. The analogous hydroxide binding constant to dinuclear Cu_2(C-BISTREN)[4] was found to be $10^{6.2}$. The polarity of the hydroxide ion explains the difference in binding constants of OH^- and F^- for dinuclear Cu_2(C-BISTREN), $10^{6.2}$ vs $10^{3.3}$, but does not account for the extremely high binding constant of OH^- for Cu_2(O-BISTREN). The very high specificity of the latter for hydroxide ion was rationalized[1,4] by predicting hydrogen bonding between the hydroxide ion and one of the ether oxygens of the cryptand ligand, indicated by **1**. This could be via an ordered or disordered arrangement. Because of the unusual nature of **1** it was considered of interest to determine its structure. A description of the structure of a crystal obtained from a solution of **1** is the subject of this report.

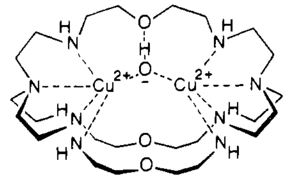

(μ-hydroxo)dicopper(II) O-BISTREN cryptate (1)

Table I. Crystallographic Parameters

empirical formula	$Cu_2Br_3N_8C_{24}O_{10}H_{67}$
fw	994.64
cryst syst	monoclinic
lattice params	$a = 15.793$ (3) Å $b = 11.100$ (5) Å $c = 24.506$ (5) Å $\beta = 90.92$ (2)° $V = 4296$ (2) Å^3
space group	*C*2/*c* (No. 15)
Z	4
D(calc)	1.54 g/cm^3
F(000)	2040
μ(Mo Kα)	40.38 cm^{-1}
transmission factors	0.66–1.00
diffractometer	Rigaku AFC5R, CONTROL software[13]
radiation	Mo Kα (λ = 0.71069 Å), graphite monochromated
temp	23 (1) °C
2θ(max) data	50.1°
no. of observns with $I > 2.00(\sigma(I))$	2551
no. of variables	341
residuals: R, R_w	0.053, 0.060
goodness of fit indicator	1.51
max shift in final cycle	0.96
largest, smallest peaks in final diff map	0.75, −0.58 e/Å^3
scan type	ω–2θ
scan width in ω	(A + 0.30 tan θ)°
scan speed in ω	16.0°/min
bkgd counting	50.0%
diam, incident beam collimeter	0.5 mm
cryst to detector dist	225.0 mm
extinction cor	0.163 e^{-6}

Experimental Section

Preparation of Crystalline $Cu_2(\mu\text{-}OH)$(O-BISTREN)Br_3. To 49 mg (0.05 mmol) of O-BISTREN hexahydrobromide[3] and 25 mg (0.10 mmol) of cupric bromide (Baker Analyzed) were added approximately 3 mL of distilled water and 7.0 mL of 0.100 N NaOH (MCB). The resulting solution was filtered, and the filtrate was allowed to evaporate to about 1.0 mL through a small opening to the atmosphere over a period of 1 week. As indicated below, the data collection crystals turned out to be hexahydrate. A solid sample taken from the main body of the reaction product proved to be the decahydrate. The elemental analysis was performed by Galbraith Laboratories, Inc. Anal. Calcd for $C_{24}H_{75}N_8O_{14}Br_3Cu_2$: C, 27.02; H, 7.08; N, 10.50; Br, 22.7. Found: C, 26.93; H, 6.03; N, 10.59; Br, 22.65.

Crystallographic Study. A crystal fragment of approximate dimensions 0.2 × 0.2 × 0.4 mm was cut from a larger crystal and mounted in random orientation on a glass fiber. Experimental conditions are reported in Table I. Cell parameters were obtained from least-squares refinement using the setting angles of 25 carefully centered reflections in the range $48.50 < 2\theta < 49.97°$. On the basis of the systematic absences of *hkl* ($h + k \neq 2n$) and *h*0*l* ($l \neq 2n$), a statistical analysis of intensity distribution, and the successful solution and refinement of the structure, the space group was determined to be *C*2/*c* (No. 15).

ω scans of several intense reflections, made prior to data collection, had an average width of 0.88°, which experimentally determined the scan value $A = (0.92°)\omega$. During data collection, the weak reflections ($I > 10.0\sigma(I)$) were rescanned a maximum of twice and the counts were accumulated to assure good counting statistics. Stationary background counts were recorded on each side of the reflection.

Of the 4195 reflections that were collected, 4032 were unique. Equivalent reflections were merged (R_{av} = 0.5%). The intensities of three representative reflections, which were measured after every 150 reflections, remained constant throughout data collection, indicating crystal

---

(1) Motekaitis, R. J.; Martell, A. E.; Lehn, J. M.; Watanabe, E. I. *Inorg. Chem.* **1982**, *21*, 4253.

(2) Motekaitis, R. J.; Martell, A. E.; Dietrich, B.; Lehn, J. M. *Inorg. Chem.* **1984**, *23*, 1588.

(3) Motekaitis, R. J.; Martell, A. E.; Murase, I. *Inorg. Chem.* **1986**, *25*, 938.

(4) Motekaitis, R. J.; Martell, A. E.; Murase, I.; Lehn, J. M.; Hosseini, M. W. *Inorg. Chem.* **1988**, *27*, 3630.

0020-1669/89/1328-0112$01.50/0

Table II. Positional Parameters and *B*(eq) Values for the (μ-Hydroxo)dicopper O-BISTREN Complex

atom	*x*	*y*	*z*	*B*(eq), Å^2
Cu	0.51267 (4)	0.23924 (6)	0.32656 (3)	2.47 (3)
N2	0.5230 (3)	0.1871 (5)	0.4062 (2)	3.1 (2)
C3	0.5241 (5)	0.2956 (6)	0.4416 (3)	3.7 (3)
C4	0.5717 (5)	0.3959 (6)	0.4144 (3)	3.5 (3)
N5	0.5330 (3)	0.4239 (4)	0.3611 (2)	2.7 (2)
C6	0.5817 (4)	0.5214 (6)	0.3337 (3)	3.3 (3)
C7	0.5284 (5)	0.5944 (6)	0.2953 (3)	3.4 (3)
O8	$^1/_2$	0.5230 (5)	$^1/_4$	4.0 (3)
C9	0.6022 (5)	0.1157 (7)	0.4133 (3)	4.0 (4)
C10	0.6251 (5)	0.0549 (6)	0.3604 (3)	3.7 (3)
N11	0.6265 (3)	0.1491 (5)	0.3179 (2)	3.0 (2)
C12	0.7061 (4)	0.2202 (7)	0.3176 (3)	3.7 (3)
C13	0.7768 (5)	0.1619 (8)	0.2862 (3)	4.3 (4)
O14	0.7556 (3)	0.1436 (4)	0.2302 (2)	4.1 (2)
C15	0.7617 (4)	0.2506 (8)	0.1977 (3)	4.3 (4)
C16	0.6721 (4)	0.2993 (7)	0.1854 (3)	3.6 (3)
N17	0.3849 (3)	0.2077 (5)	0.3362 (2)	2.9 (2)
C18	0.3685 (4)	0.1726 (7)	0.3932 (3)	3.8 (3)
C19	0.4460 (5)	0.1122 (7)	0.4166 (3)	3.7 (3)
Br1	0.37662 (8)	0.2290 (1)	0.55753 (5)	5.38 (7)
Br2	0.5729 (1)	0.0695 (1)	0.71505 (6)	6.42 (9)
Br3	0.5550 (2)	0.2118 (2)	0.5949 (1)	7.9 (2)
O100	0.1331 (3)	0.0401 (5)	0.0907 (2)	6.0 (3)
O101	0.2297 (3)	0.0640 (5)	0.5059 (2)	5.9 (3)
O102	0.7209 (4)	0.1642 (5)	0.5387 (2)	6.8 (3)
O1	$^1/_2$	0.2761 (6)	$^1/_4$	2.7 (3)
H1	0.573 (4)	−0.010 (6)	0.349 (2)	5 (2)
H2	0.468 (4)	0.325 (6)	0.449 (2)	4 (2)
H3	0.546 (4)	0.274 (6)	0.483 (3)	5 (2)
H4	0.641 (4)	0.320 (5)	0.218 (3)	3 (1)
H5	0.563 (4)	0.456 (6)	0.440 (3)	4 (2)
H6	0.674 (4)	0.361 (6)	0.161 (3)	4 (2)
H7	0.358 (4)	0.257 (5)	0.417 (3)	4 (1)
H8	0.592 (4)	0.072 (6)	0.440 (3)	4 (2)
H9	0.649 (3)	0.181 (5)	0.425 (2)	2 (1)
H10	0.722 (4)	0.224 (6)	0.357 (3)	5 (2)
H11	0.626 (3)	0.379 (5)	0.412 (2)	1 (1)
H12	0.779 (4)	0.084 (6)	0.297 (3)	4 (2)
H13	0.782 (5)	0.220 (7)	0.164 (3)	7 (2)
H14	0.634 (4)	0.480 (5)	0.311 (2)	3 (1)
H15	0.562 (3)	0.656 (5)	0.279 (2)	3 (1)
H16	0.486 (3)	0.450 (5)	0.371 (2)	2 (1)
H17	0.320 (4)	0.107 (7)	0.392 (3)	6 (2)
H18	0.463 (4)	0.041 (5)	0.397 (2)	3 (1)
H19	0.620 (4)	0.107 (6)	0.288 (3)	5 (2)
H20	0.441 (4)	0.102 (6)	0.456 (3)	5 (2)
H21	0.384 (3)	0.146 (4)	0.318 (2)	1 (1)
H22	0.704 (5)	0.298 (7)	0.305 (3)	6 (2)
H23	0.682 (4)	0.018 (5)	0.367 (2)	4 (1)
H24	0.829 (5)	0.232 (6)	0.291 (3)	7 (2)
H25	0.791 (4)	0.321 (6)	0.219 (3)	4 (2)
H26	0.603 (5)	0.588 (7)	0.365 (3)	7 (2)
H27	0.475 (5)	0.618 (6)	0.313 (3)	6 (2)
H28	$^1/_2$	0.333 (6)	$^1/_4$	1 (2)
H50	0.1268	0.1040	0.0779	6.7
H51	0.1446	0.0378	0.1112	6.7
H52	0.0935	0.0267	0.0747	6.7
H53	0.1461	0.0118	0.0748	6.7
H60	0.2707	0.0800	0.5168	6.8
H61	0.2051	0.1148	0.4859	6.8
H62	0.2449	0.0218	0.4885	6.8
H70	0.7450	0.1428	0.5555	7.7
H71	0.7472	0.2053	0.5224	7.7
H72	0.6784	0.1723	0.5547	7.7
H73	0.7230	0.1361	0.5121	7.7

and electronic stability. No decay correction was applied.

Intensity was defined as $C - {}^1/_2(t_c/t_b)(b_1 + b_2)$, where C = total number of counts, t_c = time spent counting peak intensity, t_b = time spent counting one side of the background, b_1 = high-angle background counts, and b_2 = low-angle background counts; the intensity error $\sigma(F^2) = (C + {}^1/_4(t_c/t_b)^2(b_1 + b_2) + (pI)^2)^{1/2}$, where I is the intensity and p is the factor that downweights strong reflections, taken to be 0.05. An empirical absorption correction, based on azimuthal scans of three reflections, was applied. The data were corrected for Lorentz and polarization effects. A correction for secondary extinction was applied.

Table III. Important Bond Distances (Å)

Cu–O1	1.928 (2)[a]	C7–O8	1.430 (7)
Cu–N2	2.040 (5)	C9–C10	1.51 (1)
Cu–N17	2.066 (5)	C10–N11	1.476 (8)
Cu–N11	2.071 (5)	N11–C12	1.484 (8)
Cu–N5	2.239 (5)	C12–C13	1.51 (1)
N2–C3	1.484 (8)	C13–O14	1.421 (9)
N2–C9	1.488 (9)	O14–C15	1.434 (8)
N2–C19	1.498 (8)	C15–C16	1.54 (1)
C3–C4	1.51 (1)	C16–N17	1.452 (9)
C4–N5	1.466 (8)	N17–C18	1.476 (8)
N5–C6	1.493 (8)	C18–C19	1.50 (1)
C6–C7	1.492 (9)	O1–H28	0.63 (7)

[a] Estimated standard deviations in the last significant figure are given in parentheses.

Table IV. Important Bond Angles (deg)

O1–Cu–N2	175.6 (2)[a]	C7–C6–N5	112.8 (5)
O1–Cu–N17	93.5 (2)	O8–C7–C6	110.8 (5)
O1–Cu–N11	94.6 (2)	C7–O8–C7	111.7 (7)
O1–Cu–N5	100.7 (2)	N2–C9–C10	110.5 (6)
N2–Cu–N17	84.6 (2)	N11–C10–C9	107.2 (6)
N2–Cu–N11	84.5 (2)	C10–N11–C12	113.7 (5)
N2–Cu–N5	83.6 (2)	C10–N11–Cu	104.3 (4)
N17–Cu–N11	141.4 (2)	C12–N11–Cu	118.7 (4)
N17–Cu–N5	104.3 (2)	N11–C12–C13	114.1 (6)
N11–Cu–N5	111.2 (2)	O14–C13–C12	112.8 (6)
C3–N2–C9	111.2 (5)	C13–O14–C15	113.6 (6)
C3–N2–C19	110.7 (5)	O14–C15–C16	109.2 (6)
C3–N2–Cu	109.2 (4)	N17–C16–C15	112.9 (6)
C9–N2–C19	111.6 (5)	C16–N17–C18	114.4 (6)
C9–N2–Cu	108.5 (4)	C16–N17–Cu	116.2 (4)
C19–N2–Cu	105.5 (4)	C18–N17–Cu	109.8 (4)
N2–C3–C4	110.0 (6)	N17–C18–C19	109.0 (5)
N5–C4–C3	110.4 (6)	N2–C19–C18	110.2 (5)
C4–N5–C6	110.1 (5)	H28–O1–Cu	102.3 (2)
C4–N5–Cu	101.4 (4)	Cu–O1–Cu	155.5 (4)
C6–N5–Cu	124.4 (4)		

[a] Estimated standard deviations in the last significant figure are given in parentheses.

The structure was solved by direct methods.[5] The non-hydrogen atoms were refined anisotropically. Hydrogen atoms were found by difference Fourier methods and were refined isotropically. Refinement was on F with σ weights, $1/\sigma^2(F_o)$. The final cycle of full-matrix least-squares refinement[6] gave unweighted and weighted agreement factors of $R = \sum||F_o| - |F_c||/\sum|F_o| = 0.053$ and $R_w = [\sum w(|F_o| - |F_c|)^2/\sum wF_o^2]^{1/2} = 0.060$. The standard deviation of an observation of unit weight[7] was 1.51. Plots of $\sum w(|F_o| - |F_c|)^2$ versus $|F_o|$, the reflection order in data collection, $(\sin\theta)/\lambda$, and various classes of indices showed no unusual trends. The maximum and minimum peaks on the final difference Fourier map were around the Br atoms.

Neutral-atom scattering factors were taken from Cromer and Waber.[8] Anomalous dispersion effects[9] were included in F; the anomalous dispersion terms $\Delta f'$ and $\Delta f''$ were these of Cromer.[10] All calculations were performed by using the TEXSAN[11] crystallography software package.

---

(5) Direct methods: (a) Gilmore, C. J. "MITHRIL—A Computer Program for the Automatic Solution of Crystal Structures from X-ray Data"; University of Glasgow, Glasgow, Scotland, 1983. (b) Beirskens, P. T. "DIRDIF: Direct Methods for Difference Structures—An Automatic Procedure for Phase Extension and Refinement of Difference Structure Factors"; Technical Report 1984/1; Crystallography Laboratory, Toernooiveld, 6526 Ed Nijmegen, The Netherlands.

(6) Least-squares function minimized: $\sum w(|F_o| - |F_c|)^2$, where $w = 4F_o^2/\sigma^2(F_o^2)$, $\sigma^2(F_o^2) = [S^2(C + R^2B) + (pF_o^2)^2]/(Lp)^2$, S = scan rate, C = total integrated peak count, R = ratio of scan time to background counting time, B = total background count, Lp = Lorentz–polarization factor, and p = p factor.

(7) Standard deviation of an observation of unit weight: $[\sum w(|F_o| - |F_c|)^2/(N_o - N_v)]^{1/2}$, where N_o = number of observations and N_v = number of variables.

(8) Cromer, D. T.; Waber, J. T. *International Tables for X-Ray Crystallography*; Kynoch Press: Birmingham, England, 1974; Vol. IV, Table 2.2A.

(9) Ibers, J. A.; Hamilton, W. C. *Acta Crystallogr.* **1964**, *17*, 781.

(10) Cromer, D. T. *International Tables for X-ray Crystallography*; Kynoch Press: Birmingham, England, 1974; Vol. IV, Table 2.3.1.

(11) "TEXSAN Structure Analysis Package" Molecular Structure Corp., College Station, TX, 1985 (revised 1987).

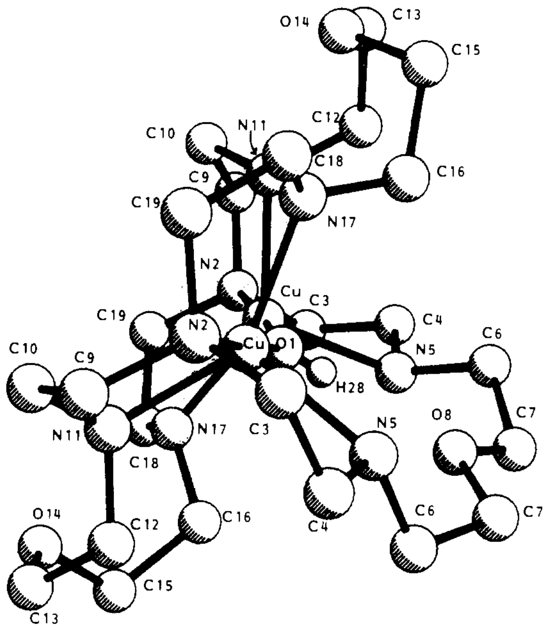

Figure 1. PLUTO representation of the (μ-hydroxo)dicopper(II) O-BISTREN structure. The 2-fold axis is along the O1–H28–O8 vector.

Final positional and equivalent isotropic thermal parameters are presented in Table II. Important bond distances are given in Table III and angles in Table IV. Anisotropic thermal parameters and structure amplitudes are provided in Tables S2 and S1 (supplementary material), respectively.

Electronic Spectroscopy. Ultraviolet–visible spectra were measured on a Perkin-Elmer Model 553 fast-scan spectrophotometer using matched 1.000-cm quartz cells.

Cu_2(O-BISTREN). A 50.0-mL solution was prepared containing 6.27 mg of O-BISTREN (6.42 × 10^{-3} mmol) and 0.546 mL of 0.02348 M $Cu(ClO_4)_2$ (12.8 × 10^{-3} mmol of Cu^{2+}), at μ = 0.100 M ($NaClO_4$). To this solution was added about 0.19 mL of 0.099 M KOH (0.019 mmol); p[H] = 4.22. Spectra were also measured at p[H] = 4.76 and 9.02.

Cu_2(TREN). Similarly, a 50-mL stock solution at μ = 0.100 M (KCl) was prepared containing 5.59 mg (0.0219 mmol) of TREN trihydrochloride and 0.930 mL of 0.02318 M $Cu(ClO_4)_2$ solution (0.0219 mmol). Spectra were measured after addition of 0.66 mL of 0.099 M KOH (p[H] = 7.94) and 1.00 mL of 0.099 M KOH (p[H] = 10.09).

Results

Figure 1 shows the geometry in a single O-BISTREN unit, while Figure 2 shows the contents of the unit cell. There is a crystallographically imposed 2-fold symmetry axis through O8 and H28. The O1–H28–O8 vector is linear, and H28–O8 is 2.11 Å, representing weak hydrogen-bond interaction. The water molecules and Br atoms form a three-dimensional hydrogen-bonding network throughout the structure. Hydrogen-bonding contacts are reported in Table V. The total bromine content is within 3 esd's of the ideal value 1.50 with occupancies for Br1 = 0.69 (5), Br2 = 0.50 (5), and Br3 = 0.46 (4). With reference to Table V it is seen that Br2 is hydrogen-bonded via N11 and N17 (3.596 (6), 3.394 (6) Å, respectively) and not to any of the water molecules. Br1 hydrogen-bonds to two symmetry-related O101 atoms (3.201 (5), 3.230 (5) Å) with the link being mostly in the *b* direction. Br3 similarly H-bonds to O100 (3.020 (6) Å) and O102 (3.025 (7) Å) primarily in the *a* and *b* directions, respectively. With reference to Figure 2 the four oxygen atoms that lie in the tunnel along the *b* axis are all hydrogen-bonded and are O100–O101–O102–O102. All these links are primarily in the *b* direction with distances 2.842 (7), 2.872 (8), and 2.85 (1) Å. The overall effect of the hydrogen-bonding scheme is to link the structure in all three directions.

Table V. Hydrogen-Bonding Contacts (Å)

	dist	ADC[a]	direction
N5–O100	3.168 (8)[b]	6	*abc*
N11–Br2	3.590 (6)	55404	*bc*
N17–Br2	3.394 (6)	65603	*b*
Br1–O101	3.201 (5)	1	*b*
Br1–O101	3.230 (5)	55607	*ab*
Br3–O100	3.020 (6)	8	*b*
Br3–O102	3.025 (7)	1	*a*
O101–O100	2.842 (7)	4	*b*
O101–O102	2.872 (8)	65603	*b*
O102–O102	2.85 (1)	65607	*b*

[a] ADC defined as for standard ORTEP drawings. Symmetry operators: (1) $+x, +y, +z$; (2) $-x, +y, {}^1/_2 - z$; (3) $-x, -y, -z$; (4) $+x, -y, {}^1/_2 + z$; (5) ${}^1/_2 + x, {}^1/_2 + y, +z$; (6) ${}^1/_2 - x, {}^1/_2 - x, {}^1/_2 - z$; (7) ${}^1/_2 - x, {}^1/_2 - y, -z$; (8) ${}^1/_2 + x, {}^1/_2 - y, {}^1/_2 + z$. [b] Estimated standard deviations in the last significant figure are given in parentheses.

Table VI. Selected p[H] Values and Corresponding Fractional Concentrations of M_2LOH, M_2L, and MH_3L

p[H]	M_2LOH	M_2L	MH_3L
4.25	0	0	0.892
4.79	0.272	0.120	0.624
9.33	1.00	0.0	0.0

Table VII. Summary of UV Absorbance Maxima for Cu(II) Complexes of O-BISTREN and TREN in Aqueous Solution[a]

ligand	complex stoichiometry	λ_1 (ϵ)	λ_2 (ϵ)
O-BISTREN	M_2LOH	270 (7973)	352 (6757)
O-BISTREN	M_2L	263 (9870)	352 (9355)
O-BISTREN	MH_3L	273 (6667)	351 (5112)
TREN	MLOH	260 (3995)	none
TREN	ML	262 (2021)	

[a] λ in nm and ϵ in cm^{-1} M^{-1}.

The orientation of the donor groups around each Cu(II) and the structure of the cavity (Figures 1 and 2) confirm the earlier suggestions[1,4] that the highest binding constant of the bridging hydroxide ion in **1** is partially due to hydrogen bonding to an ether oxygen of the cryptand ligand. Strong polarization of the O–H bond of the hydroxide ion by coordination to two Cu(II) ions should greatly increase the strength of the hydrogen bond and thus contribute to the large binding constant of the hydroxide anion.

The ultraviolet spectrum of M_2L could not be measured directly because below p[H] values of approximately 5 the dominant species is MH_3L while at higher p[H] values the major species is M_2LOH. Near p[H] = 5 the metal species present (M_2L) is

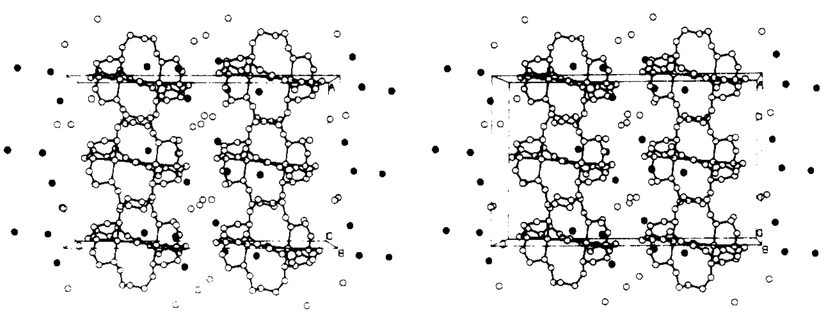

Figure 2. Stereoscopic packing diagram of $Cu_2(\mu\text{-OH})(\text{O-BISTREN})Br_3\cdot6H_2O$, shown with *c* horizontal and *a* vertical. The Br atoms are shaded; the water molecules are represented as open circles.

at its maximum but is <15%. The elusive spectrum for M_2L was computed by difference, taking into account the concentrations in Table VI, which were obtained from previously reported stability constants.

The calculations were carried out with eq 1, where ϵ values are the extinction coefficients (molar absorbances) and A_T is the observed absorbance at a given wavelength. At a given p[H],

$$\epsilon_{M_2L} = (A_T - \epsilon_{M_2LOH}[M_2LOH] - \epsilon_{MH_3L}[MH_3L])/[M_2L] \quad (1)$$

the concentration of each species was taken from Table VI, while the ϵ values for MH_3L and M_2LOH species were determined as a function of wavelength from absorbance measurements under conditions such that the only absorbing species was the complex of interest.

Discussion

The coordination geometry around each copper(II) is interesting in that the copper atoms sit just slightly above the distorted N5–N11–N17 plane, while the three N2–Cu–N angles are 84.6, 84.5, and 83.6°. The trigonal-pyramidal geometry formed by the N atoms of each moiety is mostly due to the tripodal nature of the ligand. The two TREN pockets taken together form a cavity having spacing that can adjust with apparently minimal expenditure of energy in order to accommodate the hydroxo-bridged dinuclear arrangement.

Previous solid-state ESR measurements[12] have indicated an environment of axial symmetry for the Cu(II) ions in the blue dicopper tetraperchlorate salt with considerable copper–copper interaction. The addition of water causes the ESR signal to become markedly asymmetric, as solvent entered the cavity. However, in this case, we are dealing with a μ-hydroxo complex that is characterized by a very broad, weak band at ca. 740 nm ($\epsilon = 320$) and much stronger bands at 270 ($\epsilon = 7950$) and 352 nm ($\epsilon = 6800$). Lehn and co-workers[12] reported the blue species and a green one containing O-BISTREN and 2 Cu^{2+} and 4 ClO_4^- in acetonitrile to give bands at approximately 765, 350, 283 and ca. 740, 351, 285 nm, respectively, and concluded the 350-nm band was characteristic of O-BISTREN binding, since it was absent in the Cu(II)–TREN spectra. The source of the two intense bands at short wavelength is not clear. In this work it is found that the MN_3L species also possesses two distinct peaks, in the UV–visible spectrum, even though only one TREN-like copper(II) complex is present. The peaks for MH_3L are 273 ($\epsilon = 6667$) and 351 nm ($\epsilon = 5112$).

Since the mononuclear MH_3L and the binuclear M_2L and M_2LOH species all possess similar spectra (i.e., two strong UV-visible bands), further studies should take into account all the information available from previous work on these and similar complexes. Since Cu(II)–TREN has one absorption band at 262 nm and is transparent at 350 nm, the latter band may be associated with the adjacent high positive charge (either the three alkylammonium groups in the mononuclear complex or the adjacent Cu^{2+} in the dinuclear species) in the immediate vicinity of the Cu(II) ion complexed by a TREN moiety of the ligand. Whether the presence of an anion in the cavity is essential (OH^- in Cu_2OHL or Br^- in either M_2L or MLH_3) for producing the 350-nm band is not certain, although Lehn's measurements on the dicopper(II) O-BISTREN complex with bulky perchlorate counterions seems to dismiss the possibility of such a requirement.

Now that the crystal structure of the M_2LOH complex has been determined, considerable progress can be made toward the understanding of the unique electronic spectrum of this complex. A thorough analysis of the charge involvement should be carried out, and when available, analogous complexes with similar structures should be studied. Absorbance measurements of the copper(II) complexes of C-BISTREN would address the question of the importance of hydroxide and fluoride ion binding, because hydrogen bonding of the bridging hydroxide ion is not possible in C-BISTREN complexes.

Acknowledgment. We acknowledge with thanks the Robert A. Welch Foundation for support of this work under Grants A-259 (R.J.M., A.E.M.) and A-673 (P.R.R., A.C.), and DOD Grant N00014-86-G-0194 for the single-crystal diffractometer. We express our thanks to Professor I. Murase, Kyushu University, Fukuoka, Japan, for providing the sample of O-BISTREN and to Professor J. M. Lehn, Universite Louis Pasteur, Strasbourg, France, for informative discussions.

Supplementary Material Available: A table of anisotropic thermal parameters (1 page); a table of structure factors (18 pages). Ordering information is given on any current masthead page.

---

(12) Lehn, J. M.; Pine, S. H.; Watanabe, E.; Willard, A. K. *J. Am. Chem. Soc.* **1977**, *99*, 6766.

(13) "CONTROL, an Automation Package for Rigaku AFC Single Crystal Diffractometers"; Molecular Structure Corp., College Station, TX 77840, 1986 (revised 1988).